

AD-A070 382

MASSACHUSETTS INST OF TECH LEXINGTON LINCOLN LAB  
IMAGE RESTORATION BY SHORT SPACE SPECTRAL SUBTRACTION.(U)  
FEB 79 J S LIM

F/G 5/8

UNCLASSIFIED

TN-1070-17

FSD-TP-79-27

F19628-78-C-0002

NL

OF  
AD  
A070382



END  
DATE  
FILMED

7-79  
DDC

ADA070382



MASSACHUSETTS INSTITUTE OF TECHNOLOGY  
LINCOLN LABORATORY

IMAGE RESTORATION BY SHORT  
SPACE SPECTRAL SUBTRACTION

J. S. LIM  
Group 27



TECHNICAL NOTE 1979-17

20 FEBRUARY 1979

Approved for public release; distribution unlimited.

LEXINGTON

MASSACHUSETTS

# ABSTRACT

↓  
A new image restoration system that is applicable to the problem of restoring an image degraded by blurring and additive noise is presented. ~~in this report.~~ The system is developed by attempting to estimate more accurately the frequency response of typical image restoration filters available in the literature. The resulting system combined with its short space implementation computationally simple and appears to compare quite well in performance with other restoration techniques. Some examples are given to illustrate the performance of the new image restoration system. ↗

Accession For	
NTIS GRA&I	<input checked="checked" type="checkbox"/>
DDC TAB	<input type="checkbox"/>
Unannounced	<input type="checkbox"/>
Justification	
By _____	
Distribution/ _____	
Availability Codes	
Dist	Avail and/or special
A	

## I. INTRODUCTION

A number of techniques (1,2) have been proposed in the literature to restore an image from degradations due to blurring and additive noise. Wiener filtering (3,4), parametric Wiener filtering (2), power spectrum filtering (5) and geometrical mean filtering (5) are some of the examples. In many cases, the restoration techniques are based on the assumption that an image can be modelled by a stationary random field, and restoration is achieved by filtering the degraded image with a linear space invariant restoration filter, the frequency response of which is a function of the ideal image power spectral density.

There are at least two difficulties in this approach. For a typical image, each part of an image generally differs sufficiently from other parts so that the stationarity assumption over the entire image is not generally valid. The second difficulty is that in practice, the image power spectral density is not given and has to be estimated. A common procedure used is to estimate the power spectral density by an average over different images or noise-free, blur-free prototype images whose contents are similar to the suspected content of the ideal image. Such a procedure is typically quite cumbersome, and the resulting power spectral density estimate is at best a crude approximation to the true image power spectral density. In this paper, we develop a new image restoration technique by attempting to reduce the effects of these problems.

To suggest a basis for the new restoration technique, consider an image  $f(n_1, n_2)$  degraded by additive noise and suppose that our approach is to restore the degraded image by a restoration filter such as a Wiener filter. To implement a Wiener filter, we need a good estimate of  $P_f(\omega_1, \omega_2)$ , the power spectral density of  $f(n_1, n_2)$ . A reasonable approach to obtain  $P_f(\omega_1, \omega_2)$  is to estimate it from  $f(n_1, n_2)$ . To get a good estimate of  $f(n_1, n_2)$ , however, we need a good estimate of  $P_f(\omega_1, \omega_2)$ . This then suggests

an iterative procedure in which we begin with an initial estimate of  $P_f(\omega_1, \omega_2)$  and then iteratively estimate  $f(n_1, n_2)$  and  $P_f(\omega_1, \omega_2)$  until a converging solution or a desired performance is achieved. At a first glance, this iterative procedure to estimate  $f(n_1, n_2)$  does not appear to be very useful, since many iterations may be required to obtain a converging solution and the resulting solution may be very sensitive to the initial estimate of  $P_f(\omega_1, \omega_2)$ . As will be seen later, however, with a particular method of estimating  $P_f(\omega_1, \omega_2)$  from the estimated  $f(n_1, n_2)$  and with a particular choice among existing restoration filters, a converging solution that does not depend on the initial estimate of  $P_f(\omega_1, \omega_2)$  can be obtained analytically. An image restoration technique based on this converging solution for  $f(n_1, n_2)$  will be seen to be computationally simple and to perform well as an image restoration system.

To reduce the effect of the non-stationarity problem, the restoration technique developed in this paper will be implemented on a short space basis in which an image is divided into many subimages and each subimage is restored separately and then combined. As will be discussed later and consistent with other results (1,6) in the literature, short space implementation when performed properly achieves a better system performance than the approach to process an entire image at one time.

The overall objectives of this paper are to develop a new image restoration system and illustrate its performance. In Section II, we develop a new image restoration system. In Section III, we discuss various issues related to short space implementation of the system developed in Section II. In Section IV, we discuss and illustrate various examples in which the new restoration system is applied to restore images degraded by additive noise, or blurring and additive noise.

## II. IMAGE RESTORATION BY SPECTRAL SUBTRACTION (SSIR)

The problem that we consider in this paper is to restore an image degraded by blurring and additive background noise as shown in Figure 1. The degradation model in Figure 1 can also be represented by

$$g(n_1, n_2) = f(n_1, n_2) * b(n_1, n_2) \quad (1-a)$$

$$y(n_1, n_2) = g(n_1, n_2) + d(n_1, n_2) \quad (1-b)$$

$$\text{and thus } y(n_1, n_2) = f(n_1, n_2) * b(n_1, n_2) + d(n_1, n_2) \quad (2)$$

where  $f(n_1, n_2)$  represents a digital image,

$b(n_1, n_2)$  represents a linear space invariant point spread function,

and  $d(n_1, n_2)$  represents an additive noise component.

The restoration problem to be considered is to restore  $f(n_1, n_2)$  from the degraded image  $y(n_1, n_2)$ .

The restoration problem discussed above has been studied extensively in the literature and a number of techniques have been proposed. Many of them can be viewed as a two step procedure in which  $g(n_1, n_2)$  is estimated from  $y(n_1, n_2)$  by a noise reduction system and then  $f(n_1, n_2)$  is estimated from  $\hat{g}(n_1, n_2)$  by a deblurring system. More specifically, consider the restoration system shown in Figure 2. In the figure,  $P_g(\omega_1, \omega_2)$ ,  $B(\omega_1, \omega_2)$  and  $\hat{g}(n_1, n_2)$  represent the power spectrum<sup>1</sup> of  $g(n_1, n_2)$ , the discrete space Fourier transform<sup>1</sup> of  $b(n_1, n_2)$  and the estimate of  $g(n_1, n_2)$  respectively.  $P_d(\omega_1, \omega_2)$  and  $\hat{f}(n_1, n_2)$  are similarly defined, and  $\alpha$  and  $\beta$  are constants. If  $\beta$  is unity, the restoration system in Figure 2 corresponds to the parametric Wiener filtering technique (2) and if  $\alpha$  is also unity, it reduces to the Wiener filtering technique (3). If  $\alpha$  is unity,  $\beta$  is  $\frac{1}{2}$  and  $B(\omega_1, \omega_2)$  is zero phase, the system corresponds to the power spectrum filtering

1. The definitions of these terms are given in the Appendix. See also (7).

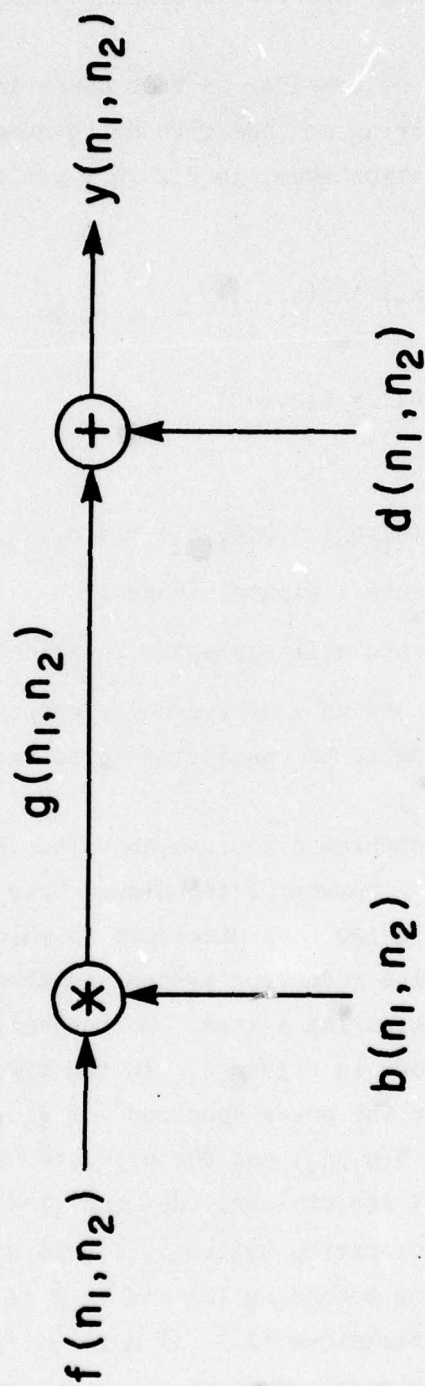


Fig. 1. Model of image degradation.

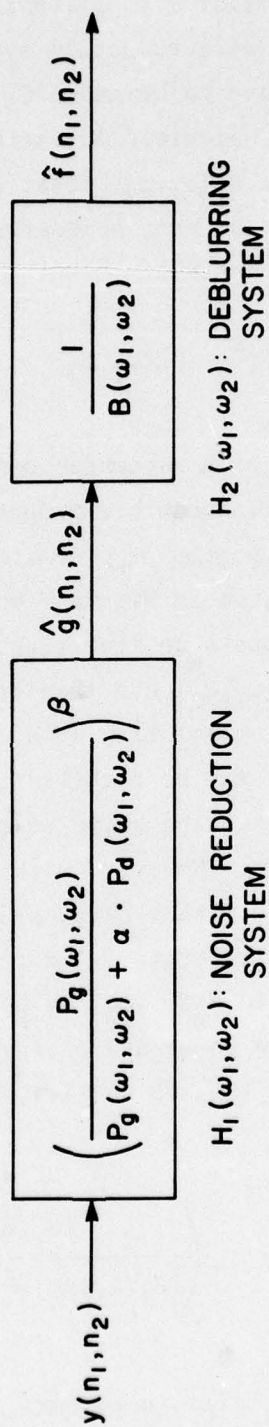


Fig. 2. An image restoration system.

technique (5). If  $\alpha$  and  $\beta$  are some constants, then the system corresponds to the geometrical mean filtering technique (2,5).

In implementing the noise reduction system  $H_1(\omega_1, \omega_2)$  in Figure 2,  $P_g(\omega_1, \omega_2)$  and  $P_d(\omega_1, \omega_2)$  have to be known<sup>2</sup>. In many cases (2), the estimation of  $P_d(\omega_1, \omega_2)$  is relatively simple. To estimate  $P_g(\omega_1, \omega_2)$ , a common procedure used is to estimate  $P_f(\omega_1, \omega_2)$  first by averaging the spectral density over many different images or over noise-free, blur-free prototype images and then using the relationship of

$$P_g(\omega_1, \omega_2) = |B(\omega_1, \omega_2)|^2 \cdot P_f(\omega_1, \omega_2) \quad (3)$$

Since different images or even subimages generally have different power spectral density, a more reasonable approach would be to estimate  $P_g(\omega_1, \omega_2)$  from  $g(n_1, n_2)$ . The function  $g(n_1, n_2)$  is not known, of course, but could be estimated by the noise reduction system in Figure 2 which requires the knowledge of  $P_g(\omega_1, \omega_2)$ . This then suggests an iterative procedure in which we begin with an initial estimate of  $P_g(\omega_1, \omega_2)$  and then iteratively estimate  $g(n_1, n_2)$  and  $P_g(\omega_1, \omega_2)$  until a converging solution or a desirable performance is achieved.

Since many iterations may be required to obtain a converging solution, the iterative procedure discussed above to estimate  $g(n_1, n_2)$  appears to be computationally undesirable. However, with a particular method of estimating  $P_g(\omega_1, \omega_2)$  from  $g(n_1, n_2)$  and with a particular choice of  $\beta$ , a simple converging solution can be analytically obtained. More specifically, suppose we let the value of  $\beta$  be  $\frac{1}{k}$  and estimate  $P_g(\omega_1, \omega_2)$  by  $\frac{1}{k}|G(\omega_1, \omega_2)|^2$  where  $k$  is a scaling factor<sup>3</sup> that normalizes the power and energy spectral densities<sup>3</sup>. Then, from Figure 2,  $\hat{g}(n_1, n_2)$  at the  $i$ th and  $i+1$ th iteration is related to each other by

$$\hat{G}_{i+1}(\omega_1, \omega_2) = Y(\omega_1, \omega_2) \cdot \left( \frac{|G_i(\omega_1, \omega_2)|^2}{|G_i(\omega_1, \omega_2)|^2 + \alpha \cdot k \cdot P_d(\omega_1, \omega_2)} \right)^{\frac{1}{2}} \quad (4)$$

2. In the literature, there exist techniques (8) in which an explicit knowledge of  $P_g(\omega_1, \omega_2)$  is not necessary. Even in such cases,  $P_f(\omega_1, \omega_2)$  still needs to be known.

3. See Appendix.

where  $Y(\omega_1, \omega_2)$  represents the discrete space Fourier transform of  $y(n_1, n_2)$ , and  $\hat{G}_i(\omega_1, \omega_2)$  and  $\hat{G}_{i+1}(\omega_1, \omega_2)$  represent the discrete space Fourier transform of  $\hat{g}(n_1, n_2)$  at the  $i$ th and  $i+1$ th iteration. If

$$\hat{G}_{i+1}(\omega_1, \omega_2) = \hat{G}_i(\omega_1, \omega_2) \quad (5)$$

then a converging solution of the iterative algorithm are reached since further iterations will produce identical results. Combining equations (4) and (5), a converging solution for  $G(\omega_1, \omega_2)$  is given by

$$\begin{aligned} \angle \hat{G}(\omega_1, \omega_2) &= \angle Y(\omega_1, \omega_2) \\ \text{and } |\hat{G}(\omega_1, \omega_2)| &= \end{aligned} \quad (6)$$

$$\begin{aligned} &\left( |Y(\omega_1, \omega_2)|^2 - \alpha \cdot k \cdot P_d(\omega_1, \omega_2) \right)^{\frac{1}{2}} \text{ if } |Y(\omega_1, \omega_2)|^2 \geq \alpha \cdot k \cdot P_d(\omega_1, \omega_2) \\ &0 \quad \text{otherwise,} \end{aligned}$$

where  $\angle G(\omega_1, \omega_2)$  and  $\angle Y(\omega_1, \omega_2)$  represent the phase of  $g(n_1, n_2)$  and  $y(n_1, n_2)$ . Equation (6) completely characterizes the new noise reduction system. The phase of  $g(n_1, n_2)$  is estimated by the phase of  $y(n_1, n_2)$  and the transform magnitude of  $g(n_1, n_2)$  is estimated by a particular form of spectral subtraction.

Combining the noise reduction system given by equation (6) with the deblurring system in Figure 2, the resulting overall image restoration system is shown in Figure 3. We'll refer to this algorithm as "Spectral Subtraction Image Restoration" (SSIR) technique. As is clear from Figure 3, the SSIR technique does not require an explicit estimation of  $P_g(\omega_1, \omega_2)$  or  $P_f(\omega_1, \omega_2)$  and the computations required for restoring an image are not any greater than typical restoration techniques such as Wiener filtering.

The SSIR technique was developed based on a converging solution of an iterative procedure that capitalizes on a particular restoration filter ( $\beta=1/2$ ) and a particular method of estimating the power spectrum of a given data. In the iterative procedure, we could, of course, have used a different

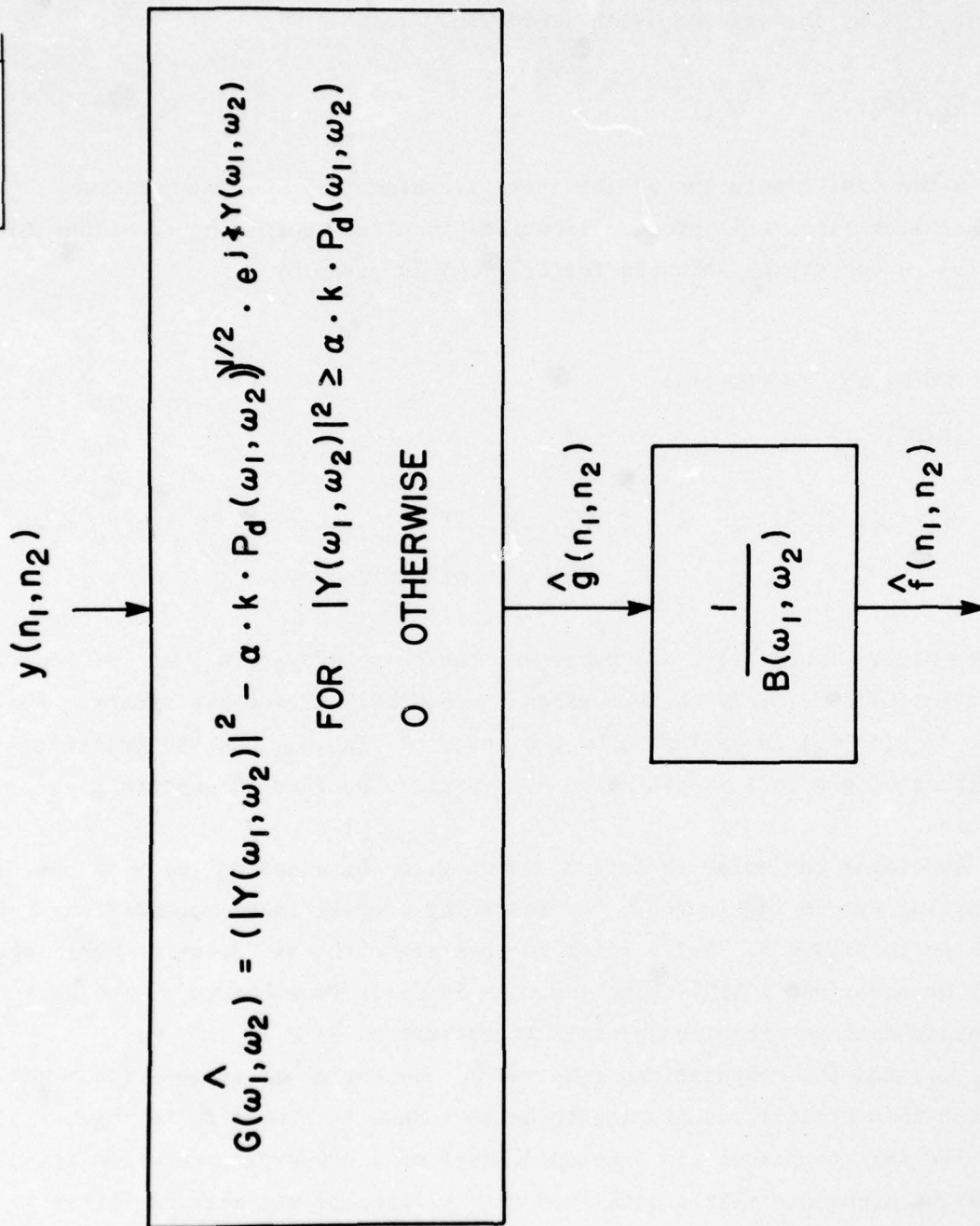


Fig. 3. Spectral subtraction image restoration technique.

value of  $\beta$  or a different method of estimating the power spectrum of a given data. In such a case, however, a converging solution cannot generally be obtained analytically and the resulting algorithm would be unattractive from the computational point of view.

### III. SHORT SPACE IMPLEMENTATION

The noise reduction system developed in the previous section is based on the assumption that  $y(n_1, n_2)$  can be approximately modelled by a stationary random field. For a typical image, each part of an image generally differs sufficiently from other parts so that the stationarity assumption is not generally valid. To reduce the effect of the non-stationarity problem, a reasonable approach is to implement the noise reduction system on a short space basis in which the degraded image is divided into many subimages and each subimage is restored separately and then combined. More specifically, we first apply a short space window function  $w_{ij}(n_1, n_2)$  to  $y(n_1, n_2)$  in equation (1-b) so that

$$y(n_1, n_2) \cdot w_{ij}(n_1, n_2) = g(n_1, n_2) \cdot w_{ij}(n_1, n_2) + d(n_1, n_2) \cdot w_{ij}(n_1, n_2). \quad (7)$$

Rewriting equation (7),

$$y_{ij}(n_1, n_2) = g_{ij}(n_1, n_2) + d_{ij}(n_1, n_2) \quad (8)$$

The noise reduction system developed in Section II is then applied to equation (8) to recover  $g_{ij}(n_1, n_2)$  from  $y_{ij}(n_1, n_2)$ .  $\hat{g}(n_1, n_2)$  is then constructed by combining  $\hat{g}_{ij}(n_1, n_2)$  as follows;

$$\hat{g}(n_1, n_2) = \sum_i \sum_j \hat{g}_{ij}(n_1, n_2) \quad (9)$$

Then the deblurring system is applied to  $\hat{g}(n_1, n_2)$  to restore  $f(n_1, n_2)$ .

To successfully implement the image restoration system on a short space basis, the window function  $w_{ij}(n_1, n_2)$  must be carefully chosen. For example, to use equation (9) in constructing an image from its subimages,  $w_{ij}(n_1, n_2)$  has to satisfy the following equation;

$$\sum_i \sum_j w_{ij}(n_1, n_2) = 1 \text{ for all } n_1, n_2 \text{ of interest} \quad (10)$$

In addition,  $w_{ij}(n_1, n_2)$  is desired to be a smooth function to avoid some possible discontinuities that may appear at the subimage boundaries in the processed image.

One way to find a smooth 2-D window function that satisfies equation (10) is to form a separable 2-D window from 1-D windows that satisfy similar conditions. For example, let  $w_x(n_1)$  and  $w_y(n_2)$  represent smooth 1-D windows with durations of  $2K$  and  $2L$  respectively;

$$w_x(n_1) = 0 \quad \text{except for } 0 \leq n_1 \leq 2K-1$$

$$w_y(n_2) = 0 \quad \text{except for } 0 \leq n_2 \leq 2L-1$$

Now let  $w_i(n_1)$  and  $w_j(n_2)$  be defined by

$$w_i(n_1) = w_x(n_1 - iK) \tag{11-a}$$

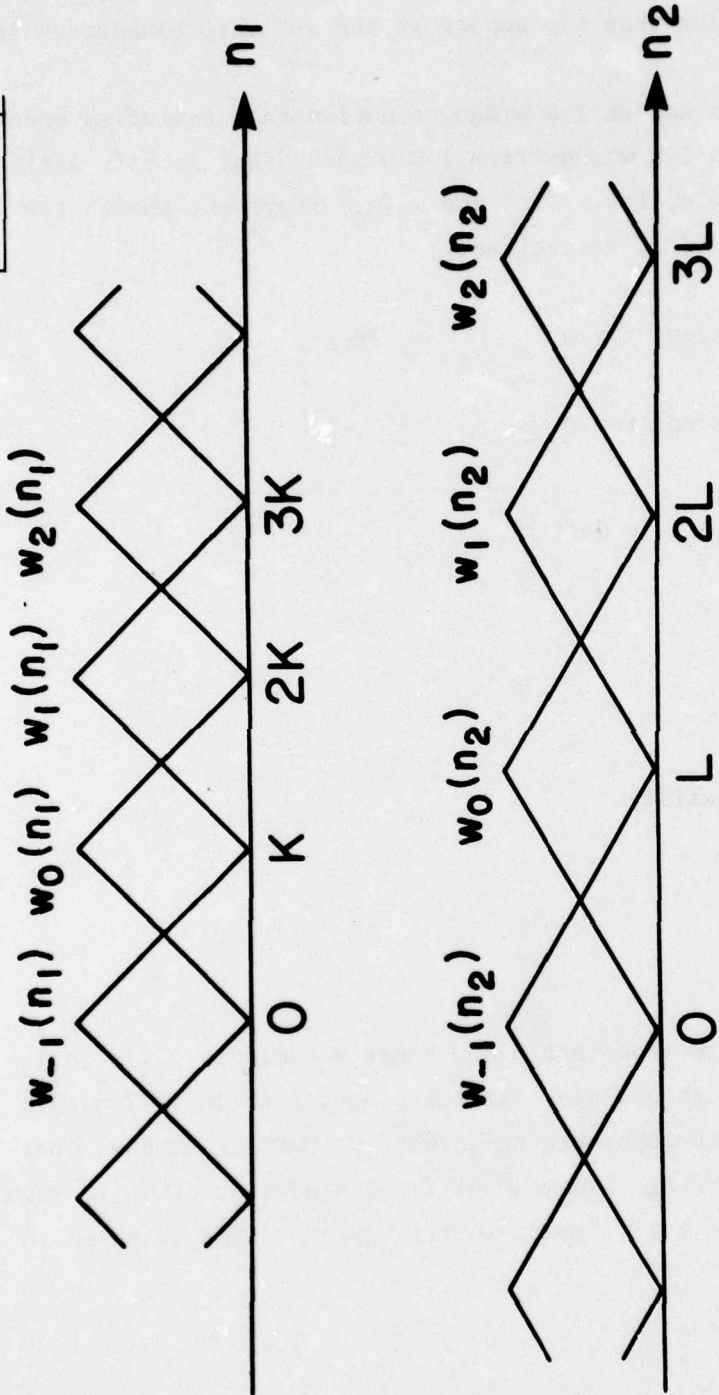
$$\text{and } w_j(n_2) = w_y(n_2 - jL). \tag{11-b}$$

If  $w_i(n_1)$  and  $w_j(n_2)$  satisfy

$$\sum_i w_i(n_1) = 1 \tag{12-a}$$

$$\text{and } \sum_j w_j(n_2) = 1, \tag{12-b}$$

it is straightforward to show that a separable 2-D window  $w_{ij}(n_1, n_2) = w_i(n_1) \cdot w_j(n_2)$  is smooth and also satisfies equation (10). Two such window functions are 2-D separable triangular or Hamming windows overlapped with its neighboring window by half the window duration in each dimension. The case of a 2-D separable triangular window is shown in Figure 4.



$$w_{ij}(n_1, n_2) = w_i(n_1) \cdot w_j(n_2)$$

Fig. 4. An example of 2-D separable triangular window.

In summary, in estimating  $g(n_1, n_2)$  from  $y(n_1, n_2)$  by the SSIR technique, we first divide  $y(n_1, n_2)$  into subimages by applying a smooth window and the noise reduction system is applied separately to each subimage. The resulting subimages are then combined to form  $\hat{g}(n_1, n_2)$  which is then deblurred to restore  $f(n_1, n_2)$ . In the next section, we illustrate the performance of the SSIR technique when applied to restore images degraded by additive noise, or blurring and additive noise.

#### IV. EXAMPLES AND DISCUSSIONS

In this section, we illustrate and discuss some examples where the short space SSIR technique developed in Sections II and III is applied to restore images degraded by additive noise, or degraded by blurring and additive noise. We first consider the case of images degraded by additive noise alone. In Figure 5 are shown two noise-free, blur-free images of 256x256 pixels with each pixel represented by 8 bits. In Figure 6 are shown two degraded images at S/N ratio of 10db which were generated by adding zero-mean white Gaussian noise to the images shown in Figure 5. The Gaussian noise was digitally generated and S/N ratio is defined by

$$\text{S/N ratio} = 10 \cdot \log \frac{\text{Variance of } f(n_1, n_2)}{\text{Variance of } d(n_1, n_2)} \quad (13)$$

In Figure 7 are shown the images restored by applying the short space SSIR technique to the noisy images in Figure 6 with  $\alpha = 2.5$  and the subimage size (window size) of 32 x 32 pixels.

The value of  $\alpha$  in the system was chosen as a compromise between noise reduction and signal distortion. If  $\alpha$  is very small, the short space SSIR technique approaches an identity system. If  $\alpha$  is very large, then large noise reduction can be achieved but at the expense of signal distortion. Based on a few other examples in addition to what are shown in this paper, we have found that a reasonable choice of  $\alpha$  at which substantial noise reduction is achieved without noticeable signal distortion is in the range of 1.5 to 3.0.

The subimage size in the short space implementation was chosen based on two considerations. If the subimage size is too large, then the non-stationarity problem that we discussed in Section III could affect the system performance. On the other hand, if the subimage size is too small, the ability of the system in reducing noise may be diminished due to lack of available data. For the types of images that we considered such as pictures of "clock" and "aerial view of a village", the subimage size in the range of

16 x 16 pixels to 32 x 32 pixels produced the best results. Consistent with the above discussions, when the SSIR technique was applied to the degraded images in Figure 6 with a too large subimage size or a too small subimage size, the system performance was not as good.

In generating the images shown in Figure 6, we used a 2-D separable triangular window discussed in Section III. Two other windows, namely 2-D separable Hamming and rectangular windows which both satisfy equation (10) were also considered. The results obtained using a Hamming window were very similar to those of a triangular window. However, the results obtained using a rectangular window had the discontinuity problem at the subimage boundaries.

Now we consider the case when images are degraded by both blurring and additive noise. In Figure 8 are shown two images obtained by first blurring the images of Figure 5 with a Gaussian shaped point spread function and then adding white Gaussian noise at S/N ratio of 20db. In Figure 9 are shown the restored images by the short space SSIR technique with  $\alpha = 2.5$  and a separable 2-D triangular window.

The value of  $\alpha$ , subimage size and window shape were again chosen based on our previous discussions. In implementing the deblurring system in Figure 3,  $|B(\omega_1, \omega_2)|$ , the magnitude of  $B(\omega_1, \omega_2)$ , was first compared to some threshold value. If the magnitude is smaller than the threshold value,  $|B(\omega_1, \omega_2)|$  was set to the threshold value without affecting the phase of  $B(\omega_1, \omega_2)$ . This step was taken to avoid possible singularity problems of inverse filtering when  $B(\omega_1, \omega_2)$  is close to zero. In general, inverse filtering accentuates the background noise and is useful only when the background noise level is very low. Thus, for example, when we performed inverse filtering on the images in Figure 8 without applying the noise reduction system, the resulting images were dominated by background noise. When accompanied by an effective noise reduction system, however, inverse filtering can be used as a deblurring system as evidenced in Figure 9.

A serious attempt has not yet been made to compare the performance of the short space SSIR technique to other restoration techniques in the literature. However, a very informal comparison was made based on several images recovered by the restoration techniques that can be represented by Figure 2. Preliminary results indicate that the performance of the restoration

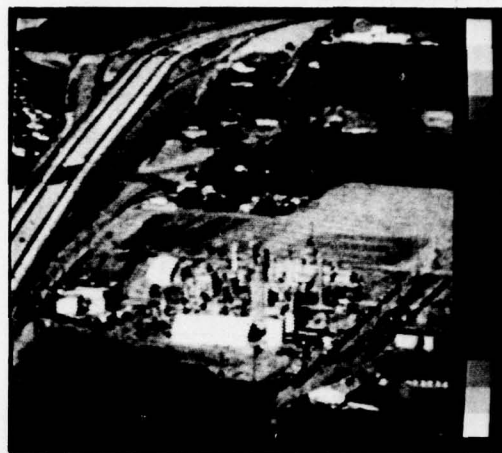
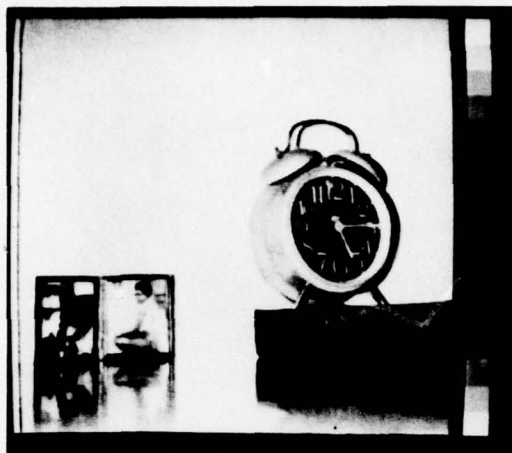


Fig. 5. Original images.

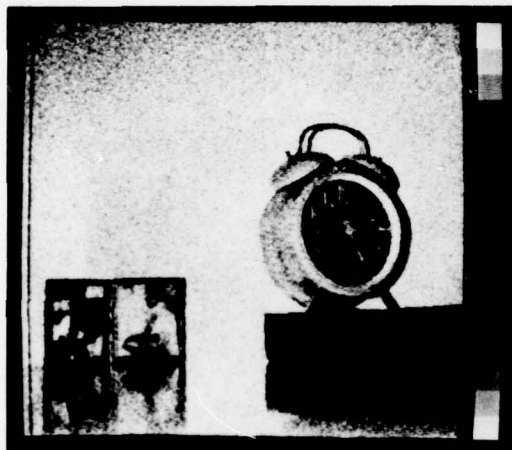


Fig. 6. Images of Fig. 5 degraded by additive noise at S/N ratio of 10 dB.

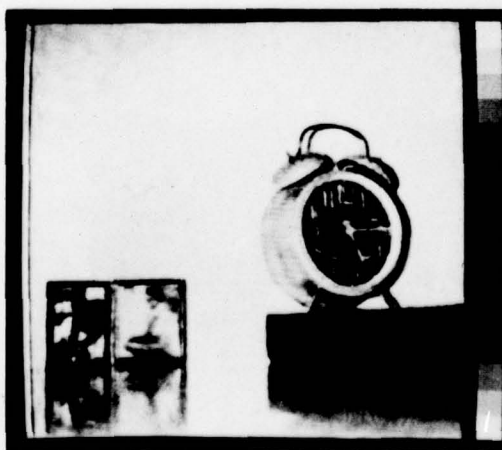


Fig. 7. Images restored from the images in Fig. 6.

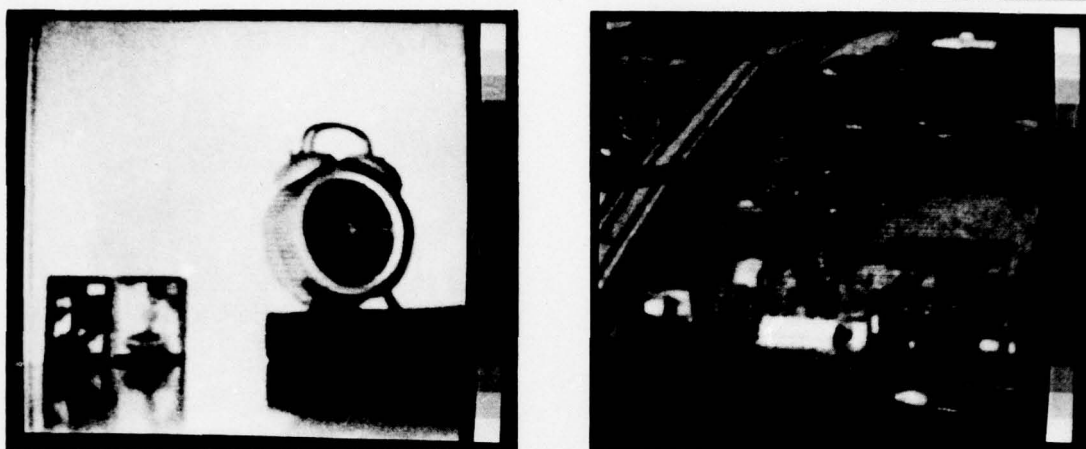


Fig. 8. Images of Fig. 5 degraded by blurring and additive noise at S/N ratio of 20 dB.

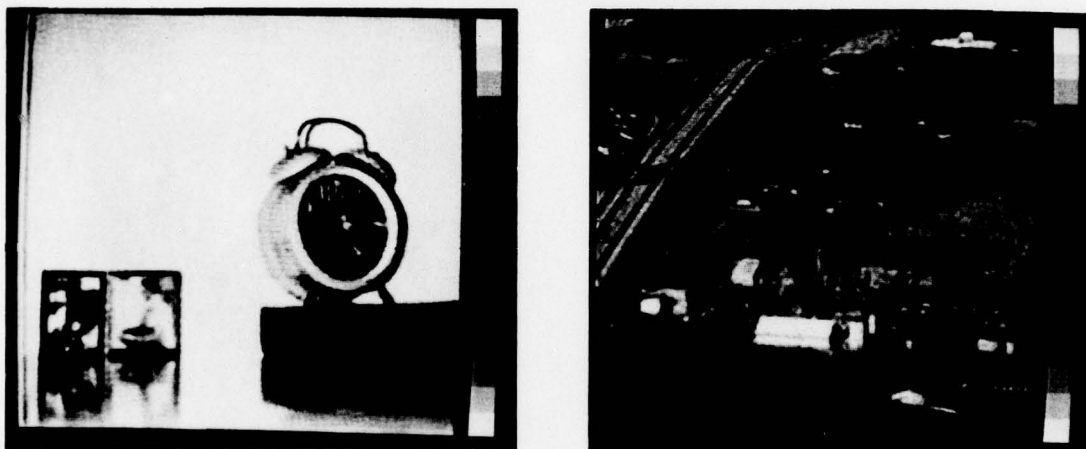


Fig. 9. Images restored from the images in Fig. 8.

*Preceding Page BLANK*

system developed in this paper compares quite well with other restoration techniques. A more detailed comparison requires further study.

Finally, in this paper we have considered short space processing for image restoration. Even though the notion of short space processing was considered in the context of a specific image restoration technique, it can also be applied to other restoration techniques. Some preliminary results indicate that short space processing based on smooth 2-D windows such as a separable triangular or Hamming window can improve the performance of other restoration techniques such as Wiener filtering.

## V. CONCLUSION

In this paper, we developed a new image restoration system which is applicable to the problem of restoring an image degraded by blurring and additive noise. The restoration system consists of a noise reduction system and a deblurring system. The main features of the noise reduction system are to estimate the spectral magnitude of the blurred image by a particular form of spectral subtraction and to implement the system on a short space basis. The deblurring system is a modification of inverse filtering. A few restoration examples were shown to illustrate the performance of the new image restoration system.

## ACKNOWLEDGEMENTS

I would like to express my appreciation to Prof. A.V. Oppenheim, Dr. S.C. Pohlig, Dr. D.E. Dudgeon and Dr. A.E. Filip for their valuable discussions and comments, and Mr. A. Gschwendtner, Dr. H. Kleiman and members of their research group at Lincoln Laboratory for making their image processing facilities available to me.

*Preceding Page BLANK - F*

## REFERENCES

- (1) W.K. Pratt, Digital Image Processing (Wiley, New York, 1978).
- (2) H.C. Andrews, B.R. Hunt, Digital Image Restoration (Prentice-Hall, Englewood Cliffs, NJ, 1977).
- (3) C.W. Helstrom, "Image Restoration by the Method of Least Squares," J. Opt. Soc. Am., 57, 297 (1967).
- (4) J.L. Horner, "Optical Spatial Filtering with the Least-Mean-Square-Error Filter," J. Opt. Soc. Am., 51, 553 (1969).
- (5) E.R. Cole, "The Removal of Unknown Image Blurs by Homomorphic Filtering," Ph.D. Dissertation, Dept. of Elec. Eng., U. of Utah, Salt Lake City (June 1973).
- (6) H.J. Trussell and B.R. Hunt, "Sectioned Methods for Image Restoration," IEEE Trans. Acoust. Speech and Signal Processing, ASSP-26, 157 (1978).
- (7) A.V. Oppenheim and R.W. Schaffer, Digital Signal Processing (Prentice-Hall, Englewood Cliffs, NJ, 1975).
- (8) T.G. Stockham, Jr., T.M. Cannon and P.V. Ingebretsen, "Blind Deconvolution through Digital Signal Processing," Proc. IEEE, 63, 678 (1975).

## APPENDIX

In the Appendix, we provide definitions for various terms used in this paper such as discrete space Fourier transform, correlation, power spectrum and energy spectrum. We also determine "k", the normalization constant used in equations (4), (6) and Figure 3.

### DEFINITIONS

$x(n_1, n_2)$ : a sample sequence of a 2-D stationary random field.

$f(n_1, n_2)$ : a finite 2-D sequence obtained by windowing  $x(n_1, n_2)$  with a rectangular window.

$$f(n_1, n_2) = 0 \text{ except for } 0 \leq n_1 \leq N_1-1 \text{ and } 0 \leq n_2 \leq N_2-1$$

$$F(\omega_1, \omega_2): \sum_{n_1=-\infty}^{\infty} \sum_{n_2=-\infty}^{\infty} f(n_1, n_2) \cdot e^{-j\omega_1 n_1} \cdot e^{-j\omega_2 n_2} = \sum_{n_1=0}^{N_1-1} \sum_{n_2=0}^{N_2-1} f(n_1, n_2) \cdot e^{-j\omega_1 n_1} \cdot e^{-j\omega_2 n_2},$$

discrete space Fourier transform of  $f(n_1, n_2)$

$|F(\omega_1, \omega_2)|^2$ : energy spectrum or periodogram of  $f(n_1, n_2)$

$R_x(n_1, n_2)$ :  $E[x(\ell_1, \ell_2) x(\ell_1 - n_1, \ell_2 - n_2)]$ , correlation of  $x(n_1, n_2)$

$$P_x(\omega_1, \omega_2): \sum_{n_1=-\infty}^{\infty} \sum_{n_2=-\infty}^{\infty} R_x(n_1, n_2) \cdot e^{-j\omega_1 n_1} \cdot e^{-j\omega_2 n_2},$$

discrete space Fourier transform of  $R_x(n_1, n_2)$  or power spectrum of  $x(n_1, n_2)$ .

# Determination of "k"

Given  $f(n_1, n_2)$ , one way to estimate  $R_x(n_1, n_2)$  is by

$$\hat{R}_x(n_1, n_2) = \frac{1}{N_1 N_2} \cdot \sum_{l_1=-\infty}^{\infty} \sum_{l_2=-\infty}^{\infty} f(l_1, l_2) \cdot f(l_1 - n_1, l_2 - n_2) \quad (A1)$$

In the frequency domain, equation (A1) is equivalent to

$$\hat{P}_x(\omega_1, \omega_2) = \frac{1}{k} \cdot |F(\omega_1, \omega_2)|^2 \quad (A2)$$

where  $k = N_1 \cdot N_2$

If  $f(n_1, n_2)$  is obtained by a more general window function  $w(n_1, n_2)$ , a straight-forward generalization of equations (A1) and (A2) are given by

$$\hat{R}_x(n_1, n_2) = \frac{1}{k} \cdot \sum_{l_1=-\infty}^{\infty} \sum_{l_2=-\infty}^{\infty} f(l_1, l_2) \cdot f(l_1 - n_1, l_2 - n_2) \quad (A3)$$

$$\text{and } \hat{P}_x(\omega_1, \omega_2) = \frac{1}{k} \cdot |F(\omega_1, \omega_2)|^2 \quad (A4)$$

$$\text{where } k = \sum_{l_1=-\infty}^{\infty} \sum_{l_2=-\infty}^{\infty} w^2(l_1, l_2) \quad (A5)$$

UNCLASSIFIED

SECURITY CLASSIFICATION OF THIS PAGE (When Data Entered)

REPORT DOCUMENTATION PAGE		READ INSTRUCTIONS BEFORE COMPLETING FORM
1. REPORT NUMBER ESD-TR-79-27	2. GOVT ACCESSION NO.	3. RECIPIENT'S CATALOG NUMBER
4. TITLE (and Subtitle) Image Restoration by Short Space Spectral Subtraction,	5. TYPE OF REPORT & PERIOD COVERED Technical Note	
7. AUTHOR(s) Jae S. Lim	8. CONTRACT OR GRANT NUMBER(s) F19628-78-C-0002	6. PERFORMING ORG. REPORT NUMBER Technical Note 1979-17
9. PERFORMING ORGANIZATION NAME AND ADDRESS Lincoln Laboratory, M.I.T. P.O. Box 73 Lexington, MA 02173	10. PROGRAM ELEMENT, PROJECT, TASK AREA & WORK UNIT NUMBERS Program Element No. 65705F Project No. 649L	
11. CONTROLLING OFFICE NAME AND ADDRESS Air Force Systems Command, USAF Andrews AFB Washington, DC 20331	12. REPORT DATE 29 February 1979	
14. MONITORING AGENCY NAME & ADDRESS (if different from Controlling Office) Electronic Systems Division Hanscom AFB Bedford, MA 01731	13. NUMBER OF PAGES 30	
15. SECURITY CLASS. (of this report) Unclassified		15a. DECLASSIFICATION DOWNGRADING SCHEDULE
16. DISTRIBUTION STATEMENT (of this Report)  Approved for public release; distribution unlimited.		
17. DISTRIBUTION STATEMENT (of the abstract entered in Block 20, if different from Report)		
18. SUPPLEMENTARY NOTES  None		
19. KEY WORDS (Continue on reverse side if necessary and identify by block number)  image restoration                      signal enhancement image enhancement                  spectral subtraction signal restoration		
20. ABSTRACT (Continue on reverse side if necessary and identify by block number)  A new image restoration system that is applicable to the problem of restoring an image degraded by blurring and additive noise is presented in this report. The system is developed by attempting to estimate more accurately the frequency response of typical image restoration filters available in the literature. The resulting system combined with its short space implementation is computationally simple and appears to compare quite well in performance with other restoration techniques. Some examples are given to illustrate the performance of the new image restoration system.		

UNCLASSIFIED

SECURITY CLASSIFICATION OF THIS PAGE (When Data Entered)

207 650

LB